Coordination chemistry of diphenylphosphinoferrocenylthioethers on cyclooctadiene and norbornadiene rhodium(i) platforms

Ekaterina Kozinets, Oleksandr Koniev, Oleg Filippov, Jean-Claude Daran, Rinaldo Poli, Elena V Shubina, Natalia V Belkova, Eric Manoury

Coordination chemistry of diphenylphosphinoferrocenylthioethers on cyclooctadiene and norbornadienerhodium(I) platforms

Ekaterina M. Kozinets,[a,b,c] Oleksandr Koniev,[a,b] Oleg A. Filippov,[c] Jean-Claude Daran,[a,b] Rinaldo Poli,[a,b,d] Elena S. Shubina,[c] Natalia V. Belkova,*[c] and Eric Manoury*[a,b]

Received (in XXX, XXX) Xth XXXXXXXXX 20XX, Accepted Xth XXXXXXXXX 20XX
DOI: 10.1039/b000000x

Complexes [RhCl(diene)(P,SR)] with chiral ferrocenyl phosphine-thioethers ligands (diene = norbornadiene, NBD, $\mathbf{1^R}$, or 1,5-cyclooctadiene, COD, $\mathbf{3^R}$; P,SR = CpFe(1,2-η^5-$C_5H_3(PPh_2)(CH_2SR)$; R = *t*Bu, Ph, Bz, Et) and the corresponding [Rh(diene)(P,SR)][BF_4] (diene = NBD, $\mathbf{2^R}$; COD, $\mathbf{4^R}$) have been synthesized from $[RhCl(diene)]_2$ and the appropriate P,SR ligand. The molecular structure of the cationic complexes $\mathbf{2^{tBu}}$, $\mathbf{4^{Ph}}$ and$\mathbf{4^{Bz}}$, determined by single-crystal X-ray diffraction, shows the expected slightly distorded square planar geometry. For the neutral chloride complexes, a combination of experimental IR and computational DFT investigations points to an equally four coordinate square planar geometry with the diene ligand, the chlorine and the phosphorus atoms in the coordination sphere and with a dangling thioether function. However, a second isomeric form featuring a 5-coordinated square planar geometry with the thioether function placed in the axial position is easily accessible in some cases.

Introduction

Since the development by Noyori and coworkers of efficient catalytic systems for the asymmetric hydrogenation of non functionalized ketones[1-3], much effort has been devoted to the asymmetric hydrogenation of polar substrates,[4] ketones[5] but also imines[6-9] or heteroarenes,[10] because of their great scientific and practical importance, which includes industrial applications.[11, 12] Most of the catalysts used so far are based on ruthenium, rhodium and iridium with phosphorus and nitrogen-containing ligands.

Our group has worked extensively on the chiral ligand platform built around the planar chirality of ferrocene, mostly with asymmetric 1,2 substitution, but also 1,2,3 trisubstitution and 1,2,3,1' tetrasubstitution.[13-17] Our interest in recent years has focused on chiral ligands based on P and S donor atoms with the development of the 1,2-substituted ferrocenes (P,SR) shown in Scheme 1.[18-22] The use of these ligands (particularly for R = Et, Ph, Bz and *t*Bu) has led to a number of catalytic applications in asymmetric allylic substitution[23, 24] asymmetric methoxycarbonylation[25] and asymmetric hydrogenation.[26] Although other kinds of ligands based on P and S donor atoms have already been used in C=C hydrogenations,[27-30] we reported the first application of these types of ligands, to the best of our knowledge, to the hydrogenation of ketones, promising results being obtained in the ionic hydrogenation of various acetophenones.[26]

In combination with $[IrCl(COD)]_2$ (COD = 1,5-cyclooctadiene), these ligands have yielded the corresponding IrCl(COD)(P,SR) adducts, of which those with R = Et, Ph and Bz adopt a 5-coordinate square pyramidal geometry (axial Cl) in the solid state and in solution, whereas the *t*Bu derivative is square planar with a dangling thioether function.[31] These iridium complexes were shown to be excellent precatalysts for the hydrogenation of aromatic ketones in the presence of a strong base such as NaOMe in methanol and other alcohols, leading to quantitative hydrogenations in less than two hours at room temperatures under 30 bar of H_2 and with only 0.05% of catalyst loading and with enantiomeric excesses that reached >99% (at 0°C) for selected substrates.[26]

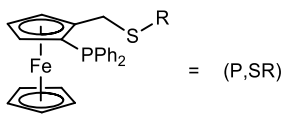

Scheme 1. General structure of the (P,SR) ligands used in this study.

Specific stoichiometric investigations of the precatalyst hydrogenation in methanol, yielding partial hydrogenation of the cyclooctadiene to cyclooctene (experimentally observed by GC-MS) and presumably leading at least initially to Ir(P,SR)(OMe)(MeOH), have not so far allowed the isolation or spectroscopic observation of a catalytically active species. It is known from elegant work by Heller *et al.* that the hydrogenation of diene ligands in complexes such as $[M(diene)(L_2)]^+$ (L_2 being typically a diphosphine ligand a M = Rh) in methanol yields $[M(L_2)(MeOH)_2]^+$ adducts and that such derivatives are less easily generated and less stable when M = Ir.[32-35] With the goal of generating more stable model complexes of the above mentioned iridium catalysts, we have therefore turned out attention to analogous Rh complexes. We report in this contribution the synthesis and characterization of a variety of adducts of the (P,SR) ligands in Scheme 1 with $[RhCl(COD)]_2$ and $[RhCl(NBD)]_2$ (NBD = norbornadiene). This includes an IR study and a DFT investigation to elucidate the structure of the compound in the solid state and in solution. Related cationic complexes $[Rh(COD)(P,SR)]^+$ and $[Rh(NBD)(P,SR)]^+$ have also been isolated and structurally characterized. We also report preliminary investigations of acetophenone hydrogenation using these rhodium complexes as precatalysts. It will be shown that, albeit the catalytic activity is lower, these complexes are good structural and functional models of the corresponding Ir precatalysts.

Experimental Section

General. All reactions were carried out under an argon atmosphere using standard Schlenk techniques. Solvents were carefully dried by conventional methods and distilled under argon before use. The (R/S)-2-diphenylphosphanyl-(R-thiomethyl)-ferrocene ligands (R = Et, *t*Bu, Ph, Bz) were prepared according to a published procedure from racemic 2-(diphenylthio-phosphanylferrocenyl)methanol.[36] Compounds $[RhCl(COD)]_2$, $[RhCl(NBD)]_2$ and $[Rh(COD)_2]BF_4$ were purchased from Strem Chemicals and used as received. ^1H, $^{13}C\{^1H\}$ and $^{31}P\{^1H\}$ NMR spectra were recorded with a Bruker Avance 500 FT-NMR spectrometer. The resonances were calibrated relative to the residual solvent peaks and are reported with positive values downfield from TMS. For all characterized compounds, the peak assignments in the ^1H and ^{13}C NMR spectra were based on COSY, HSQC and HMBC 2D experiments. HRMS were obtained from dichloromethane solutions with a Xevo G2 Q TOF spectrometer by the electrospray method. IR spectra were recorded at room temperature with a Nicolet 6700 spectrometer in the solid state (as nujol mulls) using polyethylene cells for the low frequency region. The optical purity and the conversions for the hydrogenation experiments were determined by chiral GC (Supelco BETA DEX™ 225).

General procedure for the synthesis of RhCl(NBD)(P,SR), 1. In a Schlenk tube, under nitrogen, ligand (P,SR) (0.793 mmol) was dissolved in dichloromethane (5 mL) and $[RhCl(NBD)]_2$ (183 mg, 0.396 mmol) was added. The solution was stirred for 4 h at room temperature and 15 mL of pentane was then added to yield a yellow precipitate. The precipitate was filtered under argon and washed with pentane to give RhCl(NBD)(P,SR).

RhCl(NBD)(P,S*t*Bu) (1^{tBu}, yield: 97%). ^1H NMR (500 MHz, $CDCl_3$): δ 8.48 (m, 2H, Ph); 7.53 (m, 3H, Ph); 7.3-7.2 (m, 3H, Ph); 6.93 (brdd, 2H, Ph, J_{HH} = 7.2 Hz, J_{HP} = 9.7 Hz) ; 5.06 (d (AB), 1H, C$\underline{H}_2$Fc, J_{HH} = 13.8 Hz); 4.56 (s, 1H, subst. Cp); 4.30 (s, 1H, subst. Cp); 4.14 (s, 1H, subst. Cp); 3.90 (s, 5H, Cp); 3.84 (d (AB), 1H, C$\underline{H}_2$Fc, J_{HH} = 13.8 Hz); 3.78 (s, 2H, CH NBD); 3.61 (s, 2H, CH NBD); 3.57 (s, 2H, CH NBD); 1.51 (s, 9H, *t*Bu) 1.23 (s, 2H, CH_2 NBD). $^{13}C\{^1H\}$ NMR (125 MHz, $CDCl_3$): δ 136.3 (d, Ph, J_{CP} = 12.8 Hz); 135.3 (d, quatPh, J_{CP} = 45.6 Hz); 133.8 (d, quatPh, J_{CP} = 45.6 Hz); 132.3 (d, Ph, J_{CP} = 9.2 Hz); 130.4 (d, Ph, J_{CP} = 2.2 Hz); 128.7 (d, Ph, J_{CP} = 1.8 Hz); 127.7 (d, Ph, J_{CP} = 10.4 Hz); 127.2 (d, Ph, J_{CP} = 9.2 Hz); 91.3 (d, quatCp, J_{CP} = 18.6 Hz); 73.3(s, substCp); 71.9 (d, substCp, J_{CP} = 7.6 Hz); 71.5 (d, quatCp, J_{CP} = 7.6 Hz); 71.0 (s, Cp); 69.0 (d, substCp, J_{CP} = 5.2 Hz); 61.4 (s, CH_2 NBD); 60.2(br s, CH NBD); 55.9 (br s, CH NBD); 48.5 (s, CH NBD); 46.0(s, S-C(CH$_3$)); 31.3 (s, S-C(C$\underline{H}_3$)); 28.8 (C$\underline{H}_2$Fc). $^{31}P\{^1H\}$ NMR (202 MHz, $CDCl_3$): δ 23.6 (d, $J_{P\text{-}Rh}$ = 159 Hz). MS (ESI) *m/e*: 667,081 (M-Cl$^-$, 100 %).

RhCl(NBD)(P,SPh) (1^{Ph},yield: 98%). ^1H NMR (500 MHz, $CDCl_3$): δ 8.52 (m, 2H, Ph); 7.73 (br d, J_{HH} = 7.5 Hz, 2H, Ph); 7.58 (m, 3H, Ph); 7.4-7.1 (m, 3H, Ph); 6.62 (m, 2H, Ph) ; 5.37 (br d (AB), 1H, C$\underline{H}_2$Fc, J_{HH} = 13 Hz); 4.45 (br s, 1H, subst. Cp); 4.28 (br d (AB), 1H, C$\underline{H}_2$Fc, J_{HH} = 13 Hz); 4.24 (br s, 1H, subst. Cp); 4.03 (br s, 1H, subst. Cp); 3.88 (s, 5H, Cp); 3.54 (s, 4H, CH NBD); 3.40 (s, 2H, CH NBD); 1.17 (s, 2H, CH_2 NBD). $^{13}C\{^1H\}$ NMR (125 MHz, $CDCl_3$): δ 136.2 (d, Ph, J_{CP} = 13.0 Hz); 135.3 (d, quat Ph, J_{CP} = 46.8 Hz); 135.1 (quat Ph); 133.3 (d, quat Ph, J_{CP} = 46.0 Hz); 131.6 (d, Ph, J_{CP} = 9.3 Hz); 130.6 (d, Ph, J_{CP} = 2.2 Hz); 130.3 (Ph); 129.0 (Ph); 128.6 (d, Ph, J_{CP} = 1.8 Hz); 127.9 (d, Ph, J_{CP} = 10.5 Hz); 127.5 (Ph); 127.2 (d, Ph, J_{CP} = 9.4 Hz); 89.0 (d, quat Cp, J_{CP} = 18.6 Hz); 72.6 (s, subst Cp); 72.4 (d, subst Cp, J_{CP} = 7.7 Hz); 71.0 (s, Cp); 70.8 (d, quat Cp, J_{CP} = 40 Hz); 69.1 (d, Ph, J_{CP} = 5.0 Hz); 60.8 (d, J_{CRh} = 5.3 Hz, CH_2 NBD); 59.1(d, J_{CRh} = 7.6 Hz, CH NBD); 54.2 (br s, CH NBD); 48.2 (s, CH NBD); 34.1 (C$\underline{H}_2$Fc). $^{31}P\{^1H\}$ NMR (202 MHz, $CDCl_3$): δ 23.8 (d, $J_{P\text{-}Rh}$ = 154 Hz). MS (ESI) *m/e*: 687,049 (M-Cl$^-$, 100 %).

RhCl(NBD)(P,SBz) (1^{Bz},yield: 99%). ^1H NMR (500 MHz, $CDCl_3$): δ 8.46 (m, 2H, Ph); 7.59 (m, 3H, Ph) ; 7.45-7.25 (m, 8H, Ph); 6.88 (m, 2H, Ph); 4.32 (br s, 1H, subst. Cp); 4.25 (br s, 1H, subst. Cp); 4.13 (br d (AB), 1H, C$\underline{H}_2$Fc, J_{HH} = 12 Hz); 4.08 (s, 1H, subst. Cp); 4.00 (m, 1H C$\underline{H}_2$Fc + 1H C$\underline{H}_2$Ph); 3.73 (s, 5H, Cp); 3.70 (d (AB), 1H, C$\underline{H}_2$Ph); 3.52 (br s, 4H, NBD); 3.42 (br s, 2H, NBD); 1.19 (s, 2H, CH_2 NBD). $^{13}C\{^1H\}$ NMR (125 MHz, $CDCl_3$): δ 143.4 (quat Ph); 136.0 (d, Ph, J_{CP} = 13.3 Hz); 135.5 (d, quat Ph, J_{CP} = 43.8 Hz); 134.6 (d, quat Ph, J_{CP} = 44.8 Hz); 131.4 (d, Ph, J_{CP} = 9.4Hz); 130.5 (d, Ph, J_{CP} = 2.0 Hz); 129.5 (Ph); 128.71 (Ph); 128.66 (d, Ph, J_{CP} = 1.8 Hz); 127.9 (d, Ph, J_{CP} = 10.4 Hz); 127.7 (Ph); 127.4 (d, Ph, J_{CP} = 9.1 Hz); 88.6 (d, quat Cp, J_{CP} = 19.7 Hz); 72.6 (s, subst Cp); 72.5 (d, Ph, J_{CP} = 7.6 Hz); 70.7 (s, Cp); 70.4 (d, quat Cp, J_{CP} = 38.9 Hz); 69.1 (d, subst Cp, J_{CP} = 4.7 Hz); 60.4 (s, CH_2 NBD); 53.8 (br s, CH NBD); 49.9 (br s, CH NBD); 48.1 (s, CH NBD); 40.6 (C$\underline{H}_2$Ph); 31.3 (C$\underline{H}_2$Fc). $^{31}P\{^1H\}$ NMR (202 MHz, $CDCl_3$): δ 20.3 (d, $J_{P\text{-}Rh}$ = 147 Hz). MS (ESI) *m/e*: 701,067 (M-Cl$^-$, 100 %).

RhCl(NBD)(P,SEt) (1^{Et},yield: 99%). ^1H NMR (500 MHz, $CDCl_3$): δ 8.44 (m, 2H, Ph); 7.59 (m, 3H, Ph); 7.27 (m, 3H, Ph); 6.87 (m, 2H, Ph); 4.52 (s, 1H, subst. Cp); 4.37 (br d (AB), 1H, C$\underline{H}_2$Fc, J_{HH} = 12 Hz); 4.29 (s, 1H, subst. Cp); 4.14 (s, 1H, subst. Cp); 4.06 (br d (AB), 1H, C$\underline{H}_2$Fc, J_{HH} = 12 Hz); 3.83 (s, 5H, Cp); 3.60 (br m, 4H, CH NBD); 3.42 (br s, 2H, CH NBD); 2.81 (m, 1H, C$\underline{H}_2$CH$_3$); 2.57 (m, 1H, C$\underline{H}_2$CH$_3$); 1.38 (t, 1H, CH$_3$, J_{HH} = 6.7 Hz); 1.22 (s, 2H, CH_2 NBD). $^{13}C\{^1H\}$ NMR (125 MHz, $CDCl_3$): δ 135.9 (d, Ph, J_{CP} = 13.2 Hz); 135.5 (d, quat Ph, J_{CP} = 44.3 Hz); 134.2 (d, quat Ph, J_{CP} = 44.8 Hz); 131.4 (d, Ph, J_{CP} = 9.5 Hz); 130.5 (d, Ph, J_{CP} = 2.2 Hz); 128.7 (d, Ph, J_{CP} = 1.8 Hz); 127.9 (d, Ph, J_{CP} = 10.4 Hz); 127.5 (d, Ph, J_{CP} = 9.2 Hz); 88.8 (d, quat Cp, J_{CP} = 19.4 Hz); 72.7 (s, subst Cp); 72.5 (d, subst Cp, J_{CP} = 7.7 Hz); 70.8 (s, Cp); 70.2 (d, quat Cp, J_{CP} = 38 Hz); 69.0 (d, subst Cp, J_{CP} = 4.8 Hz); 60.7 (s, CH_2 NBD); 55.3 (br s, CH NBD); 51.2 (br s, CH NBD); 48.2 (s, CH NBD); 30.8 (C$\underline{H}_2$Fc); 29.7 ((d, J_{CRh} = 3.4 Hz, C$\underline{H}_2$CH$_3$); 13.4 (CH$_3$). $^{31}P\{^1H\}$ NMR (202 MHz, $CDCl_3$): δ 21.3 (d, $J_{P\text{-}Rh}$ = 148 Hz). MS (ESI) *m/e*: 639,049 (M-Cl$^-$, 100 %).

Synthesis of [Rh(NBD)(P,S*t*Bu)]BF$_4$, 2^{tBu}.In a Schlenk tube, under nitrogen, complex RhCl(NBD)(P,S*t*Bu) (0.148 mmol) was dissolved in dichloromethane (5 mL) and 5 ml of a water solution of$NaBF_4$ (20 mg, 0.178 mmol) was added. The organic phase was separated and dried over anhydrous sodium sulfate. After solvent evaporation, [Rh(NBD)(P,S*t*Bu)]BF_4 was obtained as a yellow solid.^1H NMR (500 MHz, $CDCl_3$): δ 7.69 (m, 2H, Ph); 7.55-7.50 (m, 6H, Ph); 7.40 (m, 2H, Ph); 5.85 – 5.65 (br m, 2H, Ph, CH nbd); 4.77 (s, 1H, subst. Cp); 4.64 (s, 5H, Cp); 4.49 (m, 1H, subst. Cp); 4.35 – 4.30 (br s, 3H, CH nbd); 4.12 (m, 1H, subst. Cp); 3.96 (d (AB), 1H, C$\underline{H}_2$Fc, J_{HH} = 12.2 Hz); 3.90 – 3.70 (br s, 1H, CH nbd); 2.81 (d (AB), 1H, C$\underline{H}_2$Fc, J_{HH} = 12.2 Hz); 1.69 (br s, 2H, CH_2 nbd); 1.37 (s, 9H, *t*Bu). $^{13}C\{^1H\}$ NMR (125 MHz, $CDCl_3$): δ 134.0 (d, Ph, J_{CP} = 13.2 Hz); 132.1 (d, Ph, J_{CP} = 2.2Hz);

131.7 (d, Ph, J_{CP} = 9.9 Hz); 131.3 (d, Ph, J_{CP} = 2.4 Hz); 129.6 (dd, quat Ph, J_{CP} = 45.8 Hz); 129.5 (d, Ph, J_{CP} = 10.6 Hz); 129.0 (d, Ph, J_{CP} = 10.8 Hz); 126.0 (d, quat Ph, J_{CP} = 52.3 Hz); 85.9 (d, quat Cp, J_{CP} = 18.5 Hz); 83.8 (br s, CH nbd); 75.8 (d, subst Cp, J_{CP} = 6.8 Hz); 72.2 (s, subst Cp); 72.0 (s, CH nbd); 71.0 (s, Cp); 70.0 (br s, CH nbd); 68.9 (d, subst Cp, J_{CP} = 5.7 Hz); 67.8 (d, CH_2 nbd, $J_{C\text{-}Rh}$ = 4.4 Hz); 64.7 (d, quat. Cp, J_{CP} = 55.2 Hz); 54.8 (s, S-$\underline{C}(CH_3)$); 31.0 (s, S-C($\underline{C}H_3$)); 29.1 (d, $\underline{C}H_2Fc$, J_{CP} = 5.3 Hz. ^{31}P NMR (500202 MHz, $CDCl_3$): δ 26.1 (d, $J_{P\text{-}Rh}$ = 158 Hz). MS (ESI) *m/e*: 667,081 (M-BF_4^-, 100 %).

General procedure for the synthesis of RhCl(COD)(P,SR), 3. In a Schlenk tube, under nitrogen, ligand (P,S*t*Bu) (0.797 mmol) was dissolved in dichloromethane (5 mL) and $[RhCl(COD)]_2$ (196mg, 0.397 mmol) was added. The solution was stirred for 4 h at room temperature and 15 mL of pentane was then added to form a yellow precipitate. The precipitate was filtered under nitrogen and washed with pentane, to give [RhCl(COD)(P,SR).Only in the case of R = *t*Bu, the product could be isolated in a pure state.Yield: 64%. **R = *t*Bu.** ^1H NMR (500 MHz, $CDCl_3$): δ 8.06 (m, 2H, Ph); 7.55-7,25 (m, 8H, Ph); 4.64 (br s, 1H, subst. Cp); 4.36 (br s, 1H, subst. Cp); 4,35-4,20 (m, 2H, 1 subst. Cp + 1 $C\underline{H}_2Fc$); 4.09 (s, 5H, Cp); 3.91 (br d (AB), 1H, $C\underline{H}_2Fc$, J_{HH} = 12.9 Hz); 2.48 (m, 2H, CH_2 cod); 2.32 (m, 2H, CH_2 cod); 1.99 (m, 2H, CH_2 cod); 1.87 (m, 2H, CH_2 cod); 1.41 (s, 9H, *t*Bu). ^{13}C HNMR (125 MHz, $CDCl_3$): δ 135.1 (d, Ph, J_{CP} = 11.9 Hz); 134.4 (d, quat Ph, J_{CP} = 43.6 Hz); 133.9 (d, Ph, J_{CP} = 10.5 Hz); 133.2 (d, quat Ph, J_{CP} = 43.4 Hz); 130.1 (d, Ph, J_{CP} = 1.7 Hz); 129.5 (Ph); 127.7 (d, Ph, J_{CP} = 10.0 Hz); 127.5 (d, Ph, J_{CP} = 9.6 Hz); 90.6 (d, quat Cp, J_{CP} = 14.1 Hz); 74.6 (d, subst Cp, J_{CP} = 7.6 Hz); 74.3 (d, quat Cp, J_{CP} = 42.2 Hz); 71.3 (d, subst. Cp, J_{CP} = 6.9 Hz); 71.1 (s, Cp); 69.8 (d, substCp, J_{CP} = 7.2 Hz); 43.0 (s, S-C($\underline{C}H_3$)); 31.9 (v. br s, CH_2 cod); 31.1 (s, S-C($\underline{C}H_3$)); 30.3 (v. br s, CH_2 cod), 28.6 (br s, $\underline{C}H_2Fc$). ^{31}P NMR (202 MHz, $CDCl_3$): δ 21.0 (d, $J_{P\text{-}Rh}$ = 148 Hz). MS (ESI) *m/e*: 683,112 (M-Cl^-, 100 %).

Essential spectroscopic parameters for the other compounds: **R = Ph**: δ 28.0 (d, $J_{P\text{-}Rh}$ = 166 Hz). **R = Bz**: δ 31.1 (d, $J_{P\text{-}Rh}$ = 170 Hz). **R = Et**: δ22.8 (d, $J_{P\text{-}Rh}$ = 144 Hz).

General procedure for the synthesis of [Rh(COD)(P,SR)]BF_4, 4. In a Schlenk tube, under nitrogen, ligand (P,SR) (0.305 mmol) was dissolved in dichloromethane (5 mL) and $[Rh(COD)_2]BF_4$ (124 mg, 0.305 mmol) was added. The solution was stirred for 30 min at room temperature and 15 mL of pentane was then added to yield a yellow precipitate. The precipitate was filtered under argon and washed with pentane to give $[Rh(COD)(P,SR)]BF_4$.

[**Rh(COD)(P,S*t*Bu)]BF_4** (**4^{tBu}**, yield 99%). ^1H NMR (500 MHz, $CDCl_3$): δ 7.60 – 7.35 (m, 10H, Ph); 5.78 (br s, 2H, CH COD); 4.78 (br s, 1H, subst. Cp); 4.64 (s, 5H, Cp); 4.48 (br s, 1H, subst. Cp); 4.12 (br s, 1H, subst. Cp); 4.00 – 3.95 (m, 2H, 1H CH cod + 1H $C\underline{H}_2Fc$); 3.85 (br s, 1H, CH COD); 2.87 (m, 1H, CH_2 COD); 2.71 (m, 1H, CH_2 COD); 2.69 (d (AB), 1H, $C\underline{H}_2Fc$, J_{HH} = 12.2 Hz); 2.59 (m, 1H, CH_2 COD); 2.49 (m, 1H, CH_2 COD); 2.39 (m, 1H, CH_2 COD); 2.30 (m, 1H, CH_2 COD); 2.07 (m, 1H, CH_2 COD); 1.96 (m, 1H, CH_2 COD); 1.37 (s, 9H, tBu). $^{13}C\{^1H\}$ NMR (125 MHz, $CDCl_3$): δ 133.9 (d, Ph, J_{CP} = 12.7 Hz); 132.3 (d, Ph, J_{CP} = 2.0 Hz); 132.1 (d, Ph, J_{CP} = 9.0 Hz); 131.6 (d, Ph, J_{CP} = 2.2 Hz); 130.0 (d, ipso Ph, J_{CP} = 44.4 Hz); 129.5 (d, Ph, J_{CP} = 10.4 Hz); 128.8 (d, Ph, J_{CP} = 10.0 Hz); 125.9 (d, ipso Ph, J_{CP} = 50.6 Hz); 104.4 (dd, CH COD, J_{CP} = 9.7 Hz, J_{CRh} = 7.1 Hz); 102.1 (dd, CH COD, J_{CP} = 9.4 Hz, J_{CRh} = 6.1 Hz); 85.5 (d, ipso Cp, J_{CP} = 17.7 Hz); 82.1 (d, CH COD, J_{CRh} = 11.3 Hz); 81.3 (d, CH COD, J_{CRh} = 12.6 Hz); 76.1 (d, subst Cp, J_{CP} = 6.7 Hz); 73.1 (s, subst Cp); 71.0 (s, Cp); 69.2 (s, subst Cp, J_{CP} = 5.7 Hz); 63.2 (d, ipso Cp, J_{CP} = 56.1 Hz); 55.7 (s, S-$\underline{C}(CH_3)$); 35.7 (s, CH_2 COD); 31.5 (CH_3); 31.0 (s, CH_2 COD); 29.2 (s, $\underline{C}H_2Fc$); 28.7 (s, CH_2 COD); 27.0 (s, CH_2 COD). $^{31}P\{^1H\}$ NMR (202 MHz, $CDCl_3$): δ 23.8 (d, $J_{P\text{-}Rh}$ = 143 Hz). MS (ESI) *m/e*: 683,112 (M-BF_4^-, 100 %).

[**Rh(COD)(P,SPh)]BF_4** (**4^{Ph}**, yield: 80%). ^1H NMR (500 MHz, $CDCl_3$): δ 7.80-7.35 (m, 15H, Ph); 5.17 (m, 1H, CH COD); 4.72 (br s, 1H, subst. Cp); 4.70 (s, 5H, Cp), 4.49 (br s, 1H, subst. Cp); 4.29 (m, 1H, CH COD); 4.17 (d (AB), 1H, $C\underline{H}_2Fc$, J_{HH} = 12.3 Hz); 4.12 (m, 1H, CH COD); 4.09 (br s, 1H, subst. Cp); 4.01 (m, 1H, CH COD); 3.04 (d (AB), 1H, $C\underline{H}_2Fc$, J_{HH} = 12.3 Hz); 2.80 (m, 1H, CH_2 COD); 2.68 (m, 1H, CH_2 COD), 2.46 (m, 2H, CH_2 COD); 2.36 (m, 1H, CH_2 COD); 2.14 (m, 1H, CH_2 COD) 2.04 (m, 1H, CH_2 COD) 1.96 (m, 1H, CH_2 COD). $^{13}C\{^1H\}$ NMR (125 MHz, $CDCl_3$): δ 134.1 (d, Ph, J_{CP} = 12.7 Hz); 132.7 (Ph); 131.9 (d, Ph, J_{CP} = 9.4 Hz); 131.7 (Ph); 131.3 (Ph); 130.4 (Ph); 130.4 (d, ipso Ph, J_{CP} = 45.1 Hz); 129.9 (d, Ph, J_{CP} = 10.1 Hz); 125.9 (d, ipso Ph, J_{CP} = 49.5 Hz); 107.0 (br s, CH COD); 103.3 (dd, CH COD, J_{CP} = 9.0 Hz, J_{CRh} = 6.0 Hz); 86.2 (d, CH COD, J_{CRh} = 11.8 Hz); 84.8 (d, ipso Cp, J_{CRh} = 16.9 Hz); 84.1 (d, CH COD, J_{CRh} = 10.8 Hz); 75.9 (d, subst Cp, J_{CP} = 6.2 Hz); 72.9 (br s, subst Cp); 71.3 (br s, Cp); 69.1 (d, subst Cp, J_{CP} = 5.8 Hz); 64.6 (d, ipso Cp, J_{CP} = 55.9 Hz); 37.9 (d, $\underline{C}H_2Fc$, J_{CP} = 4.6 Hz); 34.4 (s, CH_2 COD); 30.3 (s, CH_2 COD); 30.0 (s, CH_2 COD); 27.1 (s, CH_2 COD). $^{31}P\{^1H\}$ NMR (202 MHz, $CDCl_3$): δ 22.1 (d, $J_{P\text{-}Rh}$ = 144 Hz). MS (ESI) *m/e*: 703,081 (M-BF_4^-, 100 %).

[**Rh(COD)(P,SBz)]BF_4** (**4^{Bz}**, yield 42%). ^1H NMR (500 MHz, $CDCl_3$): δ 7.70 (m, 2H, Ph); 7.60-7.50 (m, 8H, Ph); 7.34 (m, 5H, Ph) ; 5.57 (m, 2H, CH COD); 4.54 (br s, 6H, Cp + 1H subst. Cp); 4.42 (br s, 1H, subst. Cp); 4.19 (d (AB), 1H, $C\underline{H}_2Ph$, J_{HH} = 13.8 Hz); 4.13 (br s, 1H, subst. Cp); 4.03 (d (AB), 1H, $C\underline{H}_2Ph$, J_{HH} = 13.8 Hz); 3.97 (m, 2H, CH COD); 3.50 (d (AB), 1H, $C\underline{H}_2Fc$, J_{HH} = 12.5 Hz); 2.92 (m, 1H, COD), 2.76 (m, 1H, CH COD); 2.67 (d (AB), 1H, $C\underline{H}_2Fc$, J_{HH} = 12.5 Hz); 2.60 (m, 2H, CH_2 COD); 2.48 (m, 2H, CH_2 COD) 2.36 (m, 2H, CH_2 COD) 2.13 (m, 2H, CH_2 COD). $^{13}C\{^1H\}$ NMR (125 MHz, $CDCl_3$): δ 134.2 (d, Ph, J_{CP} = 12.9 Hz); 133.7 (quat Ph); 132.3 (d, Ph, J_{CP} = 9.8 Hz); 132.1 (d, Ph, J_{CP} = 2.3 Hz); 131.4 (d, Ph, J_{CP} = 2.3 Hz); 130.2 (d, quat Ph, J_{CP} = 46.2 Hz); 129.8 (d, Ph, J_{CP} = 10.5 Hz); 129.5 (Ph); 129.1 (Ph); 128.8 (d, Ph, J_{CP} = 10.11 Hz); 127.9 (d, Ph, J_{CP} = 10.4 Hz); 128.4 (Ph); 127.2 (d, quat Ph, J_{CP} =49.6 Hz); 105.8 (dd, CH COD, J_{CP} = 9.6 Hz, J_{CRh} = 7.1 Hz); 102.7 (dd, CH COD, J_{CP} = 9.9 Hz, J_{CRh} = 6.5 Hz); 85.3 (d, CH COD, J_{CRh} = 10.9 Hz); 85.1 (d, CH COD, J_{CRh} = 11.6 Hz); 75.4 (br s, subst Cp); 72.6 (br s, subst Cp); 71.4 (br s, Cp); 69.2 (br s, subst Cp); 42.6 ($\underline{C}H_2Ph$); 34.2 (d, CH_2 COD, J_{CP} = 3.5 Hz); 31.5 (d, $\underline{C}H_2Fc$, J_{CP} = 4.6 Hz); 31.0 (d, CH_2COD, J_{CP} = 3.5 Hz); 29.7 (d, CH_2 COD, J_{CP} = 3.5 Hz); 27.6 (d, CH_2 COD, J_{CP} = 3.5 Hz). $^{31}P\{^1H\}$ NMR (202 MHz, $CDCl_3$): δ 21.8 (d, $J_{P\text{-}Rh}$ = 144 Hz).

[**Rh(COD)(P,SEt)]BF_4** (**4^{Et}**, yield: 76%). ^1H NMR (500 MHz, $CDCl_3$): δ 7.77 – 7.62 (m, 2H, Ph); 7.61-7.35 (m, 8H, Ph); 5.43 (m, 1H, CH COD); 5.33 (m, 1H, CH COD); 4.74 (br s, 1H, subst. Cp); 4.65 (s, 5H, Cp); 4.48 (m, 1H, subst. Cp); 4.12 (br s, 1H,

subst. Cp); 4.06 – 3.82 (m, 3H, 2H CH cod + 1H C<u>H</u>$_2$Fc); 2.99 (m, 1H, C<u>H</u>$_2$CH$_3$); 2.92 – 2.80 (m, 1H, CH$_2$ COD); 2.80 – 2.25 (m, 5H, CH$_2$ COD); 2.70 (d (AB), 1H, C<u>H</u>$_2$Fc, J_{HH} = 12.6 Hz); 2.20 – 2.00 (m, 2H, CH$_2$ COD); 1.32 (t, 3H, CH$_3$, J_{HH} = 7.2 Hz). ^{13}C{^{1}H} NMR (125 MHz, CDCl$_3$): δ 134.2 (d, Ph, J_{CP} = 13.0 Hz); 132.3 (d, Ph, J_{CP} = 2.2 Hz); 132.0 (d, Ph, J_{CP} = 9.5 Hz); 131.5 (d, Ph, J_{CP} = 2.4 Hz); 130.2 (d, quat Ph, J_{CP} = 45.4 Hz); 129.6 (d, Ph, J_{CP} = 10.5 Hz); 128.8 (d, Ph, J_{CP} = 10.0 Hz); 129.1 (Ph); 126.5 (d, quat Ph, J_{CP} = 49.3 Hz); 104.7 (dd, CH COD, J_{CP} = 9.6 Hz, J_{CRh} = 7.3 Hz); 103.3 (dd, CH COD, J_{CP} = 10.0 Hz, J_{CRh} = 6.2 Hz); 85.8 (d, quat Cp, J_{CP} = 16.1 Hz); 84.9 (d, CH COD, J_{CRh} = 11.7 Hz); 83.9 (d, CH COD, J_{CRh} = 10.9 Hz); 75.7 (d, subst Cp, J_{CP} = 5.9 Hz); 72.6 (s, subst Cp); 71.2 (s, Cp); 69.0 (s, subst Cp, J_{CP} = 5.4 Hz); 34.6 (d, CH$_2$ COD, J_{CP} = 3.5 Hz); 32.8 (<u>C</u>H$_2$CH$_3$); 30.9 (s, CH$_2$ COD); 30.3 (d, <u>C</u>H$_2$Fc, J_{CP} = 5.1 Hz); 29.5 (s, CH$_2$ COD); Table 1.

Crystallographic data (excluding structure factors) have been deposited with the Cambridge Crystallographic Data Centre as supplementary publication no. CCDC 872062 for **2^{tBu}**, no. CCDC 872063 for **4^{Bz}**, no. CCDC 872064 for **4^{tBu}**. Copies of the data can be obtained free of charge on application to the Director, CCDC, 12 Union Road, Cambridge CB2 1EZ, UK (fax: (+44) 1223-336-033; e-mail: deposit@ccdc.cam.ac.uk).

Table 1. Crystal data and structure refinement parameters.

	2^{tBu}	**4^{Ph}**	**4^{Bz}**
Empiricalformula	$C_{34}H_{37}FePRhS, BF_4$	$C_{37}H_{37}FePRhS, BF_4, CH_2Cl_2$	$C_{38}H_{39}FePRhS, BF_4, CH_2Cl_2$
Formula weight	754.24	875.19	889.22
Temperature, K	180(2)	180(2)	180(2)
Wavelength, Å	0.71073	0.71073	0.71073
Crystal system	Orthorhombic	Orthorhombic	Triclinic
Space group	$P2_12_12_1$	$Pca2_1$	P -1
a, Å	10.663	26.321(5)	11.5390(8)
b, Å	16.983	9.652(5)	12.8367(8)
c, Å	17.435	14.209(5)	13.5655(8)
α, °	90	90	108.445(6)
β, °	90	90	101.880(5)
γ, °	90	90	98.703(5)
Volume, Å^3	3157.3	3610(2)	1813.9(2)
Z	4	4	2
Density (calc), Mg/m^3	1.587	1.610	1.628
Abs. coefficient, mm^{-1}	1.146	1.158	1.154
F(000)	1536	1776	904
Crystal size, mm^3	0.54 x 0.47 x 0.18	0.56 x 0.22 x 0.07	0.43 x 0.22 x 0.16
Theta range, °	3.02 to 27.10	2.98 to 26.36	3.12 to 26.37
Reflections collected	12237	19753	14216
Indpt reflections (R_{int})	6118 (0.0344)	7239 (0.0342)	7393 (0.0506)
Completeness, %	98.5	99.8	99.8
Absorption correction	Multi-scan	Multi-scan	Multi-scan
Max. and min. transm.	1.0 and 0.619	1.0 and 0.7726	1.0 and 0.77764
Refinement method	F^2	F^2	F^2
Data /restr./param.	6118 / 24 / 388	7250 / 1 / 442	7408 / 24 / 478
Goodness-of-fit on F^2	1.094	1.037	1.039
R1, wR2 [I>2σ(I)]	0.0381, 0.0926	0.0340, 0.0833	0.0453, 0.1227
R1, wR2 (all data)	0.0461, 0.0954	0.0399, 0.0857	0.0555, 0.1297
Flack's parameter	0.08(3)	-0.005(18)	
Residual density, e.Å^{-3}	0.959 and -1.030	0.752 and -0.587	0.868 and -1.678

Computational details. Calculations were performed with the Gaussian09 package[41] using the B3LYP hybrid functional[42, 43] under the DFT approach, since it performs better in frequency calculations. All carbon and hydrogen atoms were described with the 6-31G(d,p) basis set, whereas the 6-31++G(d,p) basis set was applied to the P, S, B, F and Cl atoms. Effective core potentials (ECP) and its associated SDD basis set[44-47] supplemented with f-

X-ray crystallography. A single crystal of each compound was mounted under inert perfluoropolyether on the tip of a cryoloop and cooled in the cryostream of either an Oxford-Diffraction XCALIBUR SAPPHIRE-I CCD diffractometer or an Agilent Technologies GEMINI EOS CCD diffractometer. Data were collected using the monochromatic MoKα radiation (λ= 0.71073). The structures were solved by direct methods (SIR97)[37]and refined by least-squares procedures on F^2 using SHELXL-97.[38] All H atoms attached to carbon were introduced in idealised positions and treated as riding on their parent atoms in the calculations. The drawing of the molecules was realised with the help of ORTEP3.[39, 40] Crystal data and refinement parameters are shown in

polarization functions (SDD(f))[48] were applied for the Rh, Ir and Fe atoms. Geometry optimizations were performed for the neutral NBD and COD complexes **1** and **3** with R = Ph and *t*Bu without any ligand simplification. Calculations were also carried out on the isolated cation of $\mathbf{2^{Ph}}$ and on the iridium analogue IrCl(COD)(P,S*t*Bu). No scaling factors were applied to the calculated low-frequency vibrations. Since the inclusion of anharmonicity effects in the case of $\mathbf{3^{tBu}}$ did not lead to any significant change in the Rh-Cl frequency values (see Supporting Information, Table S1), this method was not applied to the other calculations.

General procedure of asymmetric hydrogenation

Solution of $6.4*10^{-3}$mmol of catalyst, $3.2*10^{-2}$ mmol of CH_3ONa (5 equivs.) and 3.2 mmol of acetophenone (500 equivs.) in 2 ml of isopropanol was transferred into a 5-ml glass vial which was then placed under argon into a stainless steel autoclave. The reaction vessel was pressurized to the 30 bar of H_2 pressure and stirred with magnetic bar for 1 hour at room temperature. The reaction was stopped by release of pressure. The crude materials were obtained by purification reaction mixture by chromatography on silica using dichloromethane as an eluent. The product was finally analyzed by chiral GC.

Results and Discussion.

(a) Syntheses

The addition of the (P,SR) ligand (1 equiv per Rh atom) to a dichloromethane solution of $[RhCl(NBD)]_2$ or $[RhCl(COD)]_2$ yielded the corresponding adducts RhCl(NBD)(P,SR), $\mathbf{1^R}$, and RhCl(COD)(P,SR), $\mathbf{3^R}$, see Scheme 2. For the NBD reagent, the complete series with R = *t*Bu, Ph, Bz and Et was obtained as pure derivatives as shown by the NMR and HRMS analyses. Concerning the COD series, although all compounds could be obtained in solution as shown by the spectroscopic analyses, only the *t*Bu derivative $\mathbf{3^{tBu}}$ could be isolated as a pure product. Starting from $\mathbf{1^{tBu}}$, addition of $NaBF_4$ in dichloromethane led to the precipitation of NaCl and formation of $[Rh(NBD)(P,S{t}Bu)]BF_4$, $\mathbf{2^{tBu}}$, in sufficient purity. The complete series of the BF_4 salts containing the COD ligand, $[Rh(COD)(P,SR)]BF_4$, $\mathbf{4^R}$, on the other hand, was more conveniently obtained by addition of (P,SR) to a solution of compound $[Rh(COD)_2]BF_4$. All these were isolated in a pure state.

(b) Characterization of the $[Rh(diene)(P,SR)]^+$ salts 2 and 4

We begin the characterization section with the salts **2** and **4**, for which the analysis is more straightforward. The NMR spectra show standard ^1H, ^{13}C and ^{31}P chemical shifts and coupling patterns for the expected square planar coordination around the Rh^I center. In particular, Rh coupling is visible for selected ^{13}C resonances of the diene ligand and for the phosphine ^{31}P resonance (the latter is collected in Table 2 for all compounds).

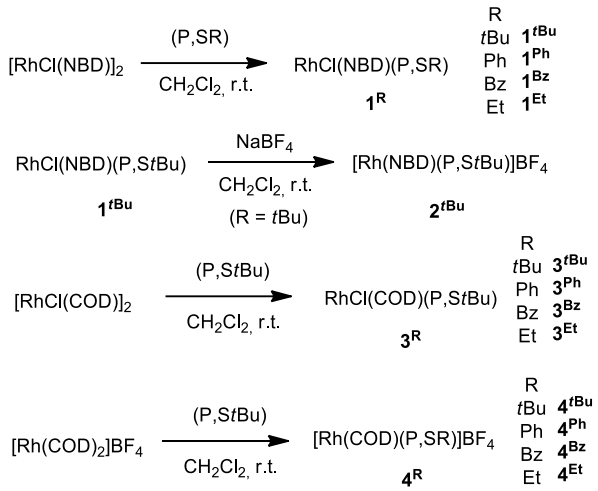

Scheme 2. Summary of the synthetic work and compounds numbering scheme.

Table 2. ^{31}P NMR data for the Rh complexes (δ in ppm with the $^2J_{PRh}$ in Hertz in parentheses).

	$\mathbf{1^R}$	$\mathbf{2^R}$	$\mathbf{3^R}$	$\mathbf{4^R}$
R = *t*Bu	23.6 (159)	26.1 (158)	21.0 (148)	23.8 (143)
R = Ph	23.8 (154)		28.0 (166)	22.1 (144)
R = Bz	20.3 (147)		31.1 (170)	21.8 (144)
R = Et	21.3 (148)		22.8 (144)	22.9 (144)

The molecular geometry of compounds $\mathbf{2^{tBu}}$, $\mathbf{4^{Ph}}$ and $\mathbf{4^{Bz}}$ was confirmed by single crystal X-ray diffraction. Whereas compound $\mathbf{2^{tBu}}$ contains only the cation and the anion in the crystal, compounds $\mathbf{4^{Ph}}$ and $\mathbf{4^{Bz}}$ crystallize with one molecule of dichloromethane per ion pair. Views of the three cations are shown in Figure 1 and relevant bond distances and angles for the three compounds are compared in Table 3. The geometry is typical of $[Rh(diene)(L^1L^2)]^+$ complexes where L^1L^2 is a chelating ligand, of which over 1000 are reported in the literature. The two midpoints of the donating ene functions and the P and S donor atoms define an approximate square planar configuration, which is quite typical of d^8 Rh^I. As a matter of fact, the geometry is nearly for $\mathbf{4^{Ph}}$, with *trans* angles quite close to 180° (P-Rh-X1 and S-Rh-X2 = 178.6(3) and 174.69(6)°, respectively; X = midpoints of the C=C bonds, see Table 3), whereas it is more distorted for $\mathbf{4^{Bz}}$. A close inspection of the structure of $\mathbf{4^{Bz}}$ shows that this distortion is related to a twist of the COD ligand, which is caused by a van der Waals repulsion between one of the COD CH=CH donating groups (C11-C12) and the CH_2 group of the benzyl substituent on sulfur (C22). A similar van der Waals repulsion, namely a 2.16Å contact between theH atoms on one of the *t*Bu methyl groups (C23) and on atom C12 of the NBD ligand, explains the even larger distortion observed in $\mathbf{2^{tBu}}$ (P-Rh-X1 and S-Rh-X2 = 163.54(4) and 166.20(4)°, respectively; see Table 3). As expected, the X1-Rh-X2 angle is much smaller for the NBD ligand with a value of 69.943(11)°, similar to the angle observed in related compound.[29] Another peculiar geometrical feature is that the sulfur substituent is placed *anti* relative to the CpFe moiety of the ferrocene group for the three complexes. Upon coordination, the sulfur atom becomes chiral and therefore two different diastereoisomers could be obtained in principle, with the sulfur substituent either *syn* or *anti* to the CpFe moiety.

Like for all previously reported complexes containing ligands of this family, without exception,[31, 49-51] a single compound is obtained in solution and the sulphur substituent is placed on the side opposite (*anti*) to the FeCp group with respect to the S-C-C-C-P chelate. Consequently, the observed diastereomer has the configuration (S_{fc}, S_S) or (R_{fc}, R_S) for $\mathbf{2}^{t\mathbf{Bu}}$and for $\mathbf{4}^{\mathbf{Ph}}$and(R_{fc}, S_S) or (S_{fc}, R_S) for $\mathbf{4}^{\mathbf{Bz}}$. The two Cp rings are roughly eclipsed with the largest twist angle, τ, 7.5(4)° for $\mathbf{4}^{\mathbf{Bz}}$.

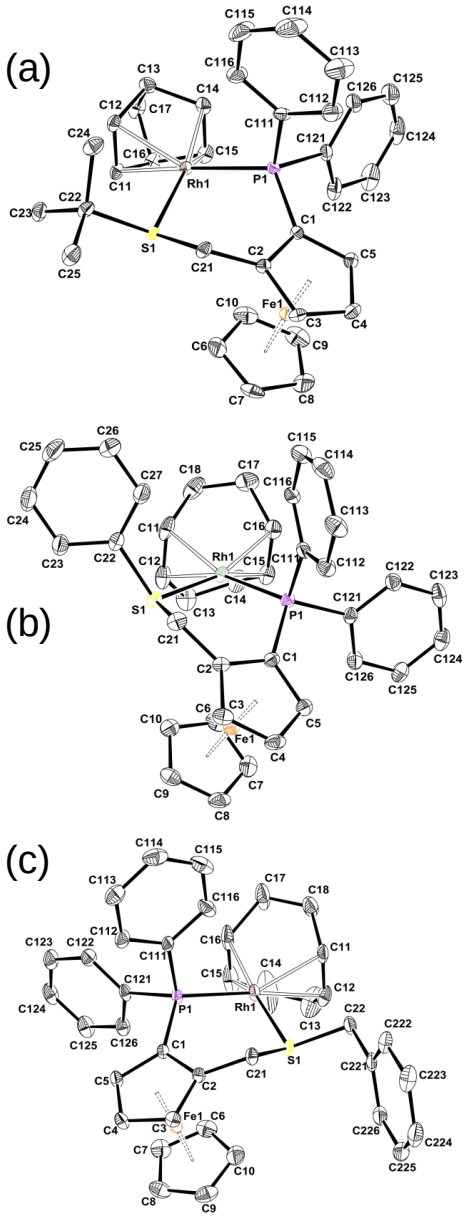

Figure 1. Molecular views of the cationic complexes in compounds $\mathbf{2}^{t\mathbf{Bu}}$ (a), $\mathbf{4}^{\mathbf{Ph}}$ (b) and $\mathbf{4}^{\mathbf{Bz}}$ (c) with the atom-labelling scheme. Displacement ellipsoids are drawn at the 30% probability level. The BF_4^- counterion and H atoms have been omitted for clarity.

A few other [Rh(diene)(P,S)]$^{n+}$ complexes of d^8 Rh^I have been previously described, some being cationic with a phosphine-thioether[28, 29, 52-55] or phosphine-phosphine sulfide[56, 57] ligand, others being neutral with a phosphine-thiolato ligand,[56, 58, 59] but the Rh-S distance does not appear to be too sensitive to this modification. The Rh-P and Rh-S distances found for $\mathbf{4}^{\mathbf{Ph}}$ and $\mathbf{4}^{\mathbf{Bz}}$ (see Table 3) compare quite well with the average in the above mentioned examples (Rh-P: 2.29(3) Å and Rh-S: 2.36(3) Å). Whereas the Rh-P distances are quite similar for the three compounds, the Rh-S distance is significantly shorter in $\mathbf{4}^{\mathbf{Bz}}$, suggesting a better binding ability of the benzyl derivative, and longer in $\mathbf{2}^{t\mathbf{Bu}}$, probably reflecting the greater steric bulk of the sulphur substituent which is also responsible for the greater geometry distortion (*vide supra*). There are no reasons to doubt that the solution structures of the other $\mathbf{4}^{\mathbf{R}}$ compounds are identical to the solid state structure found for $\mathbf{4}^{\mathbf{Ph}}$ and $\mathbf{4}^{\mathbf{Bz}}$.

DFT/B3LYP geometry optimizations were carried out for the cations of $\mathbf{2}^{\mathbf{R}}$ and $\mathbf{4}^{\mathbf{R}}$ with R = *t*Bu and Ph. The results are also reported in Table 3. For compounds $\mathbf{2}^{t\mathbf{Bu}}$ and $\mathbf{4}^{\mathbf{Ph}}$, the optimized geometry reproduced quite well the experimentally observed one, except for a slight overestimation of the Rh-P, Rh-S and Rh-C distances (by 0.08 Å on average for Rh-S and Rh-P, 0.04 Å for Rh-C). Whereas the calculated Rh-P distance is essentially the same in all four compounds, the Rh-S distance increases from Ph to the more bulky *t*Bu substituent, in agreement with the experimental evidence. Views of all optimized geometries are provided in the Supporting Information, Figure S1.

(c) Characterization of the chloride complexes 1 and 3

Concerning the neutral chlorido complexes, the solution and solid state structures cannot be assigned as easily because of the presence of five potentially coordinating ligands. We were unfortunately unable to obtain single crystals for any of these compounds, preventing us to determine the solid state structure. Interestingly, the structure adopted by the related iridium complexes IrCl(COD){CpFe[1,2-$C_5H_3(PPh_2)(CH_2SR)$]} depends on the nature of the thioether substituent.[31] For R = *t*Bu, the molecule adopts a square planar geometry with a (COD)ClP coordination environment and a dangling thioether function (*i.e.* structure **I** in Scheme 3), whereas the compounds with R = Et, Ph and Bz prefer a pentacoordinated square pyramidal geometry with a loosely bonded axial Cl ligand (structure **II**). These structural motifs seem to be maintained in solution, according to observed differences in the NMR properties, notably the ^{31}P resonance.[31] The Rh complexes $\mathbf{1}^{\mathbf{R}}$ and $\mathbf{3}^{\mathbf{R}}$ could also conceivably adopt structure **I** or **II**, but a third possibility (**III**) with a chelating (P,S) ligand and an outer sphere chloride ion, related to those observed for $\mathbf{2}^{t\mathbf{Bu}}$, $\mathbf{4}^{\mathbf{Ph}}$ and $\mathbf{4}^{\mathbf{Bz}}$ by simple replacement of the BF_4^- ion with Cl^-, can also be imagined.

Inspection of the previously published X-ray structures of related rhodium complexes suggests that **III** is unlikely but cannot be totally excluded, because a handful of compounds with the RhX(diene)(L^1L^2) stoichiometry feature indeed a free halide anion. In these structures, the cationic complex is characterized by strongly binding neutral ligands such as two monodentate N-heterocyclic carbenes (NHC),[60] a bidentatebis-NHC,[61-63] a 2,2'-bipyridine,[64] or a 2,2'-dipyridylmethane.[65] All the other structures of this type contain, like those of $\mathbf{4}^{\mathbf{Ph}}$ and $\mathbf{4}^{\mathbf{Bz}}$, non coordinating X^- anion (mostly PF_6^-, BF_4^-, $CF_3SO_3^-$ and ClO_4^-). A 5-coordinate geometry of type **II** also appears unlikely because it is much less common for Rh^I than for Ir^I, but again it cannot be excluded. Rare examples of 5-coordinate RhX(diene)(L^1L^2), with COD or NBD and including a halide ligand in the coordination geometry are limited to complexes where L^1L^2 is bipyridine,[64] 2-phenyl-

azopyridine,[64] 2-pyridylimines,[66] or an NHC-oxazoline.[67-69] It is also relevant to compare pairs of related $[Rh(diene)(L^1L^2)]^+X^-$ and $RhY(diene)(L^1L^2)$ structures (X = non coordinating anion, Y = halide), where the weaker partner of the chelating L^1L^2 donor set dissociates to let the halide enter the coordination sphere on going from the former to the latter. Examples of this situation include bidentate ligands L^1L^2 such as phosphine-amines,[70, 71] phosphine-ethers,[72] or phosphine-phosphine oxides.[73, 74] Clearly, all these examples involve a relatively strong donor (*e.g.* a phosphine) and a weaker one (N or O donor) giving the bidentate ligand a pronounced hemilability character. Apparently, examples of this type for phosphine-thioethers have not yet been described. Since no suitable single crystals for a diffraction analysis could be obtained for any of compounds **1** and **3**, their structure was addressed by a combination of spectroscopic techniques (IR, NMR) and DFT calculations.

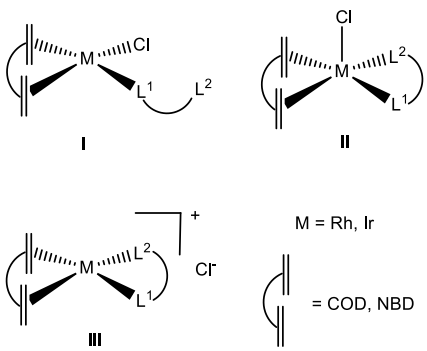

Scheme 3. Possible molecular geometries for $MCl(diene)(L^1L^2)$ complexes (M = Rh, Ir).

As shown in Table 2, the ^{31}P chemical shift and Rh coupling for compounds **1** and **3** do not greatly differ from those of the BF_4^- salts **2** and **4**. This is an expected occurrence if the chloride complexes adopted structure **III**. It should be remarked that the ^{31}P chemical shift in the $[IrCl(COD)(P,SR)]$ and $[Ir(COD)(P,SR)]^+$ compounds was found diagnostic for discriminating structures of type **I** (δ -4.2 for R = Ph and -3.1 for R = Et), **II** (δ 15.7 for R = *t*Bu) and **III** (δ 11.0 for R = Ph and 14.5 for R = *t*Bu).[31] In particular, the ^{31}P resonance is rather similar for the Ir complexes of type **II** and **III** and different relative to those with structure **I**. Therefore, the similarity between the resonances of the chloride complexes **1** and **3** with those of the BF_4 salts **2** and **4** that are known to adopt structure **III** would appear to point to a structure of type **II** or **III** for the chloride complexes. This argument, however, can in no way be considered conclusive because the metal nature may have a different effect on the chemical shift of the different structural types.

Another useful comparison comes from the detailed analysis of the ^1H spectra. Most protons (*i.e.* diene, PPh_2) are not expected to greatly respond to the structural type. The $FcC\mathit{H}_2S$ protons, on the other hand, may be sensitive to the thioether coordination, namely discriminate between **I** and **II**/**III**. The two protons of this group, whether the S atom is coordinated or not, are diastereotopic and therefore always give rise to an AB pattern. This feature was also observed for the free ligands and for the sulfur-protected version of the free ligand, (S=P,SR),[23] the ^1H and ^{13}C resonances of which are collected in Table 4 together with those of the isolated compounds **1-4**. It can be noted that the two doublets of the AB pattern in the ^1H NMR are very close to each other in the (P,SR) and (S=P,SR) molecules ($\Delta\delta < 0.4$ ppm). This difference is systematically much greater for the cationic complexes in the BF_4^- salts where the S atom is coordinated to the Rh centre (0.83 ppm in $\mathbf{4^{Bz}}$ and > 1 ppm for all other examples). It can be argued that the enantioselective sulfur coordination makes a further magnetic discrimination of the two CH_2 protons, thereby increasing their chemical shift difference. Considering now the chlorido derivatives, we note that three of them exhibit a small chemical shift difference (0.13 for $\mathbf{1^{Bz}}$, 0.31 for $\mathbf{1^{Et}}$, ca. 0.3 for $\mathbf{3^{tBu}}$), whereas the Δδ values are much greater for the other

Table 3. Selected experimental (from X-ray diffraction) and computed (by DFT optimizations) bond lengths [Å] and angles [°] in compounds $2^R$and 4^R.

	$\mathbf{2^{tBu}}$		$\mathbf{2^{Ph}}$	$\mathbf{4^{tBu}}$	$\mathbf{4^{Ph}}$		$\mathbf{4^{Bz}}$
	X-ray	**DFT**	**DFT**	**DFT**	**X-ray**	**DFT**	**X-ray**
Distances[a]							
Rh-P	2.2587(13)	2.331	2.343	2.354	2.2858(15)	2.354	2.2796(10)
Rh-S	2.3641(13)	2.452	2.402	2.508	2.3378(11)	2.421	2.3194(10)
Rh-X1	2.1231(3)	2.165	2.145	2.179	2.119(2)	2.184	2.1198(3)
Rh-X2	2.0066(4)	2.032	2.047	2.062	2.040(5)	2.069	2.0199(3)
Rh-C11	2.229(5)	2.263	2.260	2.302	2.227(4)	2.310	2.210(4)
Rh-C12	2.229(5)	2.283	2.248	2.270	2.227(4)	2.271	2.240(4)
Rh-C15	2.118(5)	2.159	2.169	2.173	2.169(4)	2.182	2.127(5)
Rh-C16	2.127(5)	2.141	2.159	2.183	2.142(4)	2.188	2.142(5)
C11-C12	1.358(8)	1.409	1.404	1.408	1.368(8)	1.404	1.352(8)
C15-C16	1.384(8)	1.383	1.385	1.384	1.391(7)	1.385	1.380(11)
Angles[a]							
P-Rh-S	92.64(5)	92.2	92.6	90.3	92.30(3)	90.9	93.24(4)
P-Rh-X1	163.54(4)	165.6	168.8	175.8	178.6(3)	177.2	168.29(3)
P-Rh-X2	93.84(13)	97.6	99.6	92.5	93.01(6)	93.5	91.59(3)
S-Rh-X1	103.01(3)	102.0	98.5	93.1	88.83(12)	91.0	90.95(3)
S-Rh-X2	166.20(4)	163.5	166.1	171.6	174.69(6)	172.6	168.21(3)
X1-Rh-X2	69.943(11)	69.2	69.6	84.4	85.87(17)	84.9	86.423(13)

[a]X1 and X2 are the midpoints of the coordinating COD C=C functions, C11-C12 and C14-C15 (for the NBD complexes) or C15-C16 (for the COD complexes), respectively.

Table 4. Selected ^{1}H (Δδ in parentheses) and ^{13}C NMR (in italics) data for the Fc*CH*$_2$S group in complexes 1-4 (δ in ppm).

	$\mathbf{1^R}$	$\mathbf{2^R}$	$\mathbf{3^R}$	$\mathbf{4^R}$	(P,SR)[a]	(S=P,SR)[a]
R = *t*Bu	5.06, 3.84 (1.22) *28.8*	3.96, 2.81 (1.15) *29.1*	ca. 4.2, 3.91 (ca. 0.3) *28.6*	ca. 4.0, 2.69(ca. 1.3) *29.2*	3.80, 3.63 (0.17) *27.4*	3.99, 3.96 (0.04) *26.7*
R = Ph	5.37, 4.2 (1.09) *34.1*			4.17, 3.04(1.15) *37.9*	4.17, 4.09 (0.08) *34.2*	4.42, 4.35 (0.07) *33.3*
R = Bz	4.13, 4.00 (0.13) *31.3*			3.50, 2.67 (0.83) *31.5*	3.72, 3.65 (0.07) *31.1*	4.14, 3.77 (0.37) *30.5*
R = Et	4.37, 4.06 (0.31) *30.8*			ca. 4.0, 2.70 (ca. 1.3) *30.3*	3.74, 3.74 (0.00) *30.9*	4.09, 3.87 (0.22) *30.3*

[a] Data from ref. [23].

two compounds (1.22 for $\mathbf{1^{tBu}}$, 1.09 for $\mathbf{1^{Ph}}$) and comparable to those of the cationic complexes. These results would tend to suggest that the thioether function is not coordinated to the Rh center in complexes $\mathbf{1^{Bz}}$, $\mathbf{1^{Et}}$ and $\mathbf{3^{tBu}}$ (*e.g.* structure **I**), whereas coordination might occur for the other two derivatives. Analysis of the Fc*CH*$_2$S ^{13}C chemical shift does not bring any additional clarification, since this resonance appears to be very little sensitive to the chemical environment as shown in Table 4.

Since the NMR analysis does not allow an unambiguous assignment of the chemical structure for the chlorido derivatives, additional studies were carried out by solid state IR spectroscopy, although limited to the COD-(P,S$^{t\mathrm{Bu}}$) and NBD-(P,S$^{t\mathrm{Bu}}$) derivatives. Spectra in the lower fingerprint region (600-250 cm^{-1}) were measured for $\mathbf{1^{tBu}}$, $\mathbf{2^{tBu}}$, $\mathbf{3^{tBu}}$, $\mathbf{4^{tBu}}$ and IrCl(COD)(P,S*t*Bu) in the solid state and the results are reported in Figure 2. The M-Cl stretching region shows various bands, the most intense one having a higher frequency for the iridium compound IrCl(COD)(P,S*t*Bu) (295 cm^{-1}) than for the rhodium compounds $\mathbf{1^{tBu}}$ and $\mathbf{3^{tBu}}$ (271 and 288 cm^{-1}, respectively). The assignment of these bands to the Ir-Cl and Rh-Cl stretching vibrations, respectively, was confirmed by the calculations (*vide infra*). On going to the tetrafluoroborate salts $\mathbf{2^{tBu}}$ and $\mathbf{4^{tBu}}$, the major band disappears in agreement with the removal of the Cl$^-$ ligand from the metal coordination sphere. These observations are in favor of a coordination geometry of type **I** or **II** (Scheme 3).

Geometry optimizations for all three types of structures were carried out at the same computational level as for the cationic complexes described above. The calculations were carried out for complexes $\mathbf{1^R}$ and $\mathbf{3^R}$ for R = *t*Bu and Ph in order to evaluate the effect of the R substituent and the diene ligand. The geometry of the iridium analogue IrCl(COD)(P,S*t*Bu) was also optimized and was found to agree quite well with that obtained experimentally in the solid state.[31] A table with the most significant metric parameters for all optimized structures is reported in the Supporting Information (Table S2). All attempts to optimize the geometry of [Rh(diene)(P,SR)]$^+$ with Cl$^-$ as a counteranion (*e.g.* a geometry of type **III** in Scheme 3) led to the dissociation of the thioether arm to allow formation of the rhodium-chloride bond (*i.e.* an optimized geometry of type **I** in Scheme 3). The geometry of the only local energy minimum obtained for $\mathbf{3^{tBu}}$ is quite similar to that of the iridium analogue, with the sulfur atom far away from the Rh center (5.556 Å).[31] Similar optimized geometries are also adopted by the other complexes ($\mathbf{1^{Ph}}$, $\mathbf{1^{tBu}}$, $\mathbf{3^{Ph}}$). Replacement of the S atom in the coordination sphere of $\mathbf{2^R}$ or $\mathbf{4^R}$ by the Cl atom in $\mathbf{1^R}$ or $\mathbf{3^R}$systematically lengthens the M-P bond by ca. 0.05 Å (*cf.* Table 3 and Table S2).

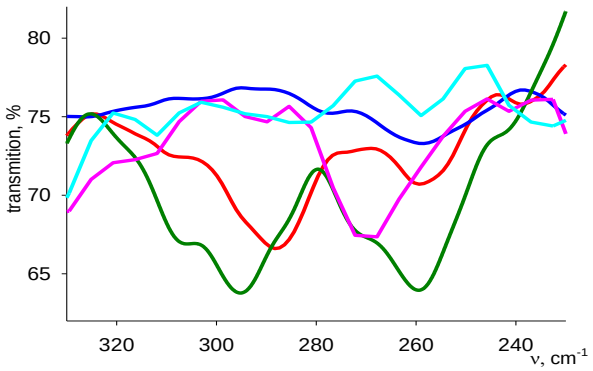

Figure 2. Solid state IR spectra (lower fingerprint region) of $\mathbf{3^{tBu}}$ (red line), $\mathbf{4^{tBu}}$ (blue line), $\mathbf{1^{tBu}}$ (pink line), $\mathbf{2^{tBu}}$ (cyan line) and IrCl(COD)(P,S*t*Bu) (green line).

A second, higher energy minimum was also found for complexes $\mathbf{1^{Ph}}$, $\mathbf{1^{tBu}}$ and $\mathbf{3^{Ph}}$. In these structures, the sulfur donor function has rearranged to place itself along the z direction perpendicularly to the square plane defined by the other four ligands, loosely interacting with the metal center, defining a pseudo pentacoordinated square-pyramidal geometry like that of **II** in Scheme 3, except that the axial coordination position of the square pyramid is occupied by the sulfur atom instead of the Cl atom (type **II'**). An example is shown in Figure 3 for compound $\mathbf{1^{tBu}}$ (all other optimized geometries are available in the Supporting Information section, Figure S2). The Rh-S distance is too long to be considered an interaction for compound $\mathbf{3^{Ph}}$ (3.674 Å), whereas it signals a genuine 5-coordinate geometry for $\mathbf{1^{Ph}}$ (2.824 Å) and $\mathbf{1^{tBu}}$ (2.702 Å), when considering that the axial interaction for 5-coordinate square pyramidal d^8 complexes is lengthened by the d_{z2} electron pair. The shorter Rh-S separation for the *t*Bu derivative may be related to the greater donating power of the S*t*Bu donor function. On the other hand, this geometry is more destabilized relative to the square planar global minimum for $\mathbf{1^{tBu}}$ (by 8.2 kcal/mol) than for $\mathbf{1^{Ph}}$ (3.1 kcal/mol). The greater steric bulk of the *t*Bu group may be responsible for this difference. All attempts to optimize a type **II** geometry led to one of the above mentioned minima. Therefore, the geometry optimizations are in favor of a structure of type **I** for compounds **1** and **3**, irrespective of the nature of the R substituent (at least for Ph and *t*Bu).

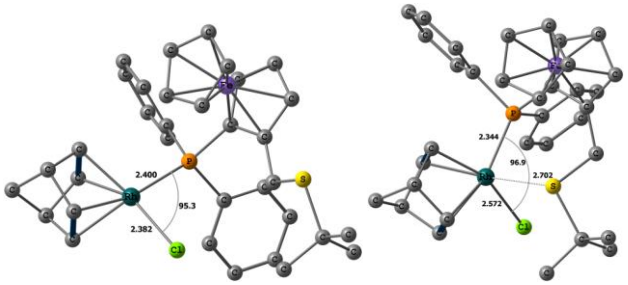

Type I (0.0) **Type II' (8.2)**

Figure 3. DFT(B3LYP) optimized geometries of 1^{Ph} with relative energies in parentheses in kcal/mol. Hydrogen atoms are omitted for clarity.

It is now of interest to analyze the calculated IR spectrum of the observed minima and compare it with the experimental ones reported in Figure 2. The M-Cl stretching vibration is coupled with M-(diene) stretches in all rhodium complexes and contributes mostly to two intense bands, which exhibit a greater frequency difference in the COD series. The analysis is rather simple for the COD compound $\mathbf{3}^{t\mathbf{Bu}}$ and for the iridium analogue, since only a minimum of type **I** was optimized. The computed spectra for these two compounds, as well as for the salt $\mathbf{4}^{t\mathbf{Bu}}$, are shown in Figure 4. These spectra match rather closely those experimentally observed, confirming the Type I structure. The calculated maximum absorption for the strongest M-Cl stretching band is at 279 cm^{-1} for the Ir complex and at 277 cm^{-1} for the Rh complex $\mathbf{3}^{t\mathbf{Bu}}$, whereas the spectrum of $\mathbf{4}^{t\mathbf{Bu}}$ does not show any strong band in this region. The adoption of a structure of type I by compound $\mathbf{3}^{t\mathbf{Bu}}$ is also in line with the suggestion of the ^{1}H NMR spectrum (AB pattern of the CH_2S*t*Bu moiety, *vide supra*).

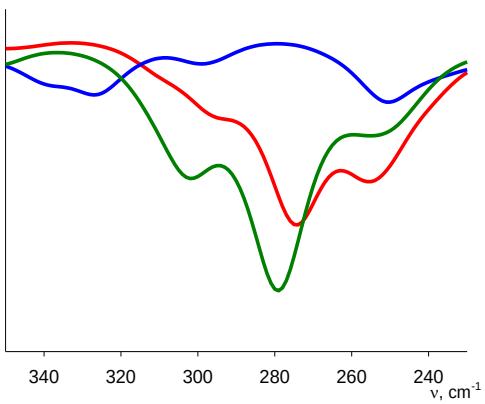

Figure 4. Calculated IR spectra (lower fingerprint region) of $\mathbf{3}^{t\mathbf{Bu}}$ (red line), $\mathbf{4}^{t\mathbf{Bu}}$ (blue line) and IrCl(COD)(P,S*t*Bu) (green line).

The calculated spectra for the type I and type II' minima of compounds $\mathbf{1}^{t\mathbf{Bu}}$and $\mathbf{1}^{\mathbf{Ph}}$ are shown in Figure 5. It can be seen that the Rh-Cl stretching band for the type I minima is very similar to that of compound $\mathbf{3}^{t\mathbf{Bu}}$ (286 and 273 cm^{-1} for the strongest absorption). On the other hand, the Rh-Cl vibration is shifted to much lower frequencies in the type II' minima of $\mathbf{1}^{\mathbf{Ph}}$ (247 cm^{-1}), and especially of $\mathbf{1}^{t\mathbf{Bu}}$ (208 cm^{-1}). This effect can obviously be attributed to the coordination of the sulfur atom, which provides additional electron density to the metal center and labilizes the Rh-Cl bond, an effect which is stronger for the *t*Bu derivative where the Rh-S distance is shorter. In agreement with this argument, the Rh-Cl distance is shorter for the type I minima of compounds $\mathbf{1}^{t\mathbf{Bu}}$ and $\mathbf{1}^{\mathbf{Ph}}$ (2.382 and 2.390 Å, respectively) and longer for the type II' geometries of $\mathbf{1}^{\mathbf{Ph}}$ (2.459 Å) and particularly $\mathbf{1}^{t\mathbf{Bu}}$ (2.572 Å). The difference between the calculated Rh-Cl frequencies for the type I and II' minima (Δν) is 78 cm^{-1} for $\mathbf{1}^{t\mathbf{Bu}}$ and 26 cm^{-1} for $\mathbf{1}^{\mathbf{Ph}}$. On the other hand, the experimental Rh-Cl stretching frequency in $\mathbf{1}^{t\mathbf{Bu}}$ is only 17 cm^{-1} lower than that of compound $\mathbf{3}^{t\mathbf{Bu}}$. Therefore, we conclude that the structure adopted by compound $\mathbf{1}^{t\mathbf{Bu}}$ is most likely of type I in the solid state, like that of compound $\mathbf{3}^{t\mathbf{Bu}}$. However, the large chemical shift difference for the CH_2S*t*Bu AB resonances in the ^{1}H NMR spectrum suggests that a structure of type II' might be more favorable in solution for this compound. If this is the case, the difference is certainly a consequence of the lower steric encumbrance of the norbornadiene ligand relative to cyclooctadiene.

The calculated spectra of compounds $\mathbf{1}^{\mathbf{Ph}}$ and $\mathbf{3}^{\mathbf{Ph}}$ (shown in the Supporting Information, Figure S3) exhibit similar features, with the major bands in the 260-280 cm^{-1} range for the type I structures and in the 240-270 cm^{-1} range for the type II' structures.

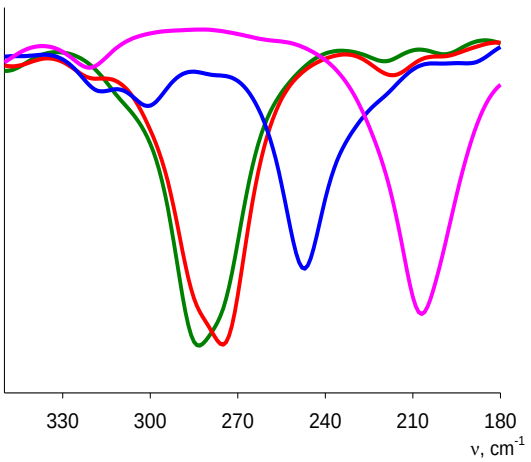

Figure 5. Calculated IR spectra (lower fingerprint region) of $\mathbf{1}^{t\mathbf{Bu}}$ type **I** (green line), $\mathbf{1}^{\mathbf{Ph}}$ type **I** (red line), $\mathbf{1}^{t\mathbf{Bu}}$ type **II'** (pink line) and $\mathbf{1}^{\mathbf{Ph}}$ type **II'** (blue line).

(d) Catalytic studies

Because iridium complexes of diphenylphosphinoferrocenyl thioether ligands were shown to be excellent precatalysts for the hydrogenation of acetophenone in the presence of NaOMe in isopropanol at room temperature under 30 bar of H_2 and with only 0.2% of catalyst, we decided to study the catalytic properties of corresponding rhodium complexes in the same conditions and compare the activity of the complexes (Scheme 4). For these preliminary investigations, we selected only the complexes with t-butyl substituent on sulfur. The results are shown in Table 5.

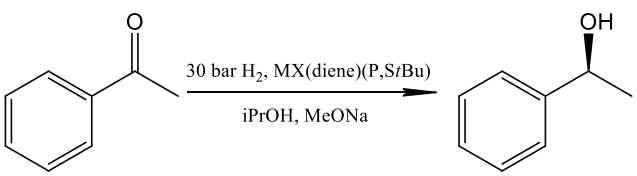

Scheme 4. Asymmetric hydrogenation of acetophenone.

Table 5. Catalytic activity of the complexes

Catalyst	Time [h]	Conversion [%]	ee (S) [%]
(S)-IrCl(COD)(P,S*t*Bu)	1	93	61
(S)-RhCl(COD)(P,S*t*Bu)	1	11	67
(S)-RhCl(NBD)(P,S*t*Bu)	1	12	46
(S)- Rh(COD)(P,S*t*Bu)BF_4	1	12	51
(S)-Rh(NBD)(P,S*t*Bu)BF_4	1	8	49

All the tested rhodium complexes are active precatalysts for the hydrogenation of acetophenone supporting our hypothesis that the rhodium complexes are not only structural but also functional models of the iridium analogues. All these rhodium complexes exhibit a rather similar catalytic activity, which is however significantly lower than that of the corresponding iridium complex IrCl(COD)(P,S*t*Bu), whereas their enantioselectivities are only slightly lower. A full description of the catalytic performance of these complexes, including the effect of the sulphur substituent, reaction temperature, and substrate, which is currently being investigated, will be reported in due course.

Conclusions

Rhodium complexes associating chiral ferrocenyl phosphine-thioethers and diene (COD or NBD) ligands have been synthesized and fully characterized. For the neutral chlorido complexes, for which X-ray structural analyses could not be carried out, combination of NMR and IR spectroscopy and DFT calculations indicates that they adopt a square planar geometry with a dangling thioether function. A second, pentacoordinated structure with a square pyramidal geometry and the thioether function placed in the axial position is however easily accessible. The cationic complexes, on the other hand adopt a standard square planar bis-chelated structure. These rhodium complexes are not only good structural models for our previously published iridium-based hydrogenation catalysts but have also been tested in the asymmetric hydrogenation of acetophenones and proved to be efficient precatalysts.

Acknowledgement

We are grateful to the CNRS (Centre National de la RechercheScientifique) and the RFBR (Russian Foundation for Basic Research) for support through the GDRI (Groupe de RechercheInternationale) “Homogeneous catalysis for Sustainable Development” and a France-Russia (RFBR - CNRS) bilateral grant. We are also grateful to the IUF (InstitutUniversitaire de France) for additional funding and to the CINES(Centre Informatique National de l'EnseignementSupérieur) and the CICT (Centre Interuniversitaire de Calcul de Toulouse, project CALMIP) for granting free computational time. EMK thanks the Embassy of France in Moscow for a Ph.D. grant.

Notes and references

[a]*CNRS, LCC (Laboratoire de Chimie de Coordination), 205 route de Narbonne, BP 44099, F-31077 Toulouse Cedex 4, France CNRS. Fax: +33-561553003; Tel: +33-561333174; E-mail: eric.manoury@lcc-toulouse.fr.*

[b]*Université de Toulouse, UPS, INPT, F-31077 Toulouse Cedex 4, France*

[c]*A. N. Nesmeyanov Institute of Organoelement Compounds, Russian Academy of Sciences, Vavilov Street 28, 119991 Moscow, Russia; Fax: +7-499-1355085; Tel:+7-499-1356448; E-mail: nataliabelk@ineos.ac.ru.*

[d] *Institut Universitaire de France, 103, bd Saint-Michel, 75005 Paris, France.*

† Electronic Supplementary Information (ESI) available: [details of any supplementary information available should be included here]. See DOI: 10.1039/b000000x/

‡ Footnotes should appear here. These might include comments relevant to but not central to the matter under discussion, limited experimental and spectral data, and crystallographic data.

1. M. Kitamura, T. Ohkuma, S. Inoue, N. Sayo, H. Kumobayashi, S. Akutagawa, T. Ohta, H. Takaya and R. Noyori, *J. Am. Chem. Soc.*, 1988, **110**, 629-631.
2. T. Ohkuma, H. Ooka, S. Hashiguchi, T. Ikariya and R. Noyori, *J. Am. Chem. Soc.*, 1995, **117**, 2675-2676.
3. R. Noyori and T. Ohkuma, *Angew. Chem. Engl.*, 2001, **40**, 40-73.
4. H. U. Blaser, C. Malan, B. Pugin, F. Spindler, H. Steiner and M. Studer, *Advanced Synthesis & Catalysis*, 2003, **345**, 103-151.
5. R. Malacea, R. Poli and E. Manoury, *Coord. Chem. Rev.*, 2010, **254**, 729-752.
6. W. Tang and X. Zhang, *Chemical Reviews (Washington, DC, United States)*, 2003, **103**, 3029-3069.
7. T. C. Nugent and M. El-Shazly, *Advanced Synthesis & Catalysis*, 2010, **352**, 753-819.
8. N. Fleury-Bregeot, V. de la Fuente, S. Castillon and C. Claver, *ChemCatChem*, 2010, **2**, 1346-1371.
9. J. H. Xie, S. F. Zhu and Q. L. Zhou, *Chem. Rev.*, 2011, **111**, 1713-1760.
10. D.-S. Wang, Q.-A. Chen, S.-M. Lu and Y.-G. Zhou, *Chem. Rev. (Washington, DC, U. S.)*, 2012, **112**, 2557-2590.
11. H.-U. Blaser, *Advanced Synthesis & Catalysis*, 2002, **344**, 17-31.
12. H. U. Blaser, B. Pugin, F. Spindler and M. Thommen, *Acc. Chem. Res.*, 2007, **40**, 1240-1250.
13. G. Iftime, J. Daran, E. Manoury and G. Balavoine, *Organometallics*, 1996, **15**, 4808-4815.
14. G. Iftime, C. MoreauBossuet, E. Manoury and G. Balavoine, *Chem. Commun.*, 1996, 527-528.
15. G. Iftime, J. Daran, E. Manoury and G. Balavoine, *Angew. Chem., Int. Ed. Eng.*, 1998, **37**, 1698-1701.
16. E. Manoury, J. Fossey, H. Ait-Haddou, J. Daran and G. Balavoine, *Organometallics*, 2000, **19**, 3736-3739.
17. J. Chiffre, Y. Coppel, G. Balavoine, J. Daran and E. Manoury, *Organometallics*, 2002, **21**, 4552-4555.
18. A. M. Masdeu-Bulto, M. Dieguez, E. Martin and M. Gomez, *Coord. Chem. Rev.*, 2003, **242**, 159-201.
19. M. Mellah, A. Voituriez and E. Schulz, *Chem. Rev.*, 2007, **107**, 5133-5209.
20. H. Pellissier, *Tetrahedron*, 2007, **63**, 1297-1330.
21. R. Malacea and E. Manoury, in *Phosphorus Ligands in Asymmetric Catalysis*, ed. A. Börner, Wiley-VCH, Weinheim, Germany, 2008, vol. 1-3, pp. 749-784.
22. F. L. Lam, F. Y. Kwong and A. S. C. Chan, *Chem. Commun.*, 2010, **46**, 4649-4667.
23. L. Routaboul, S. Vincendeau, J.-C. Daran and E. Manoury, *Tetrahedron: Asymmetry*, 2005, **16**, 2685-2690.
24. L. Routaboul, S. Vincendeau, C. O. Turrin, A. M. Caminade, J. P. Majoral, J. C. Daran and E. Manoury, *J. Organomet. Chem.*, 2007, **692**, 1064-1073.
25. L. Diab, M. Gouygou, E. Manoury, P. Kalck and M. Urrutigoity, *Tetrahedron Lett.*, 2008, **49**, 5186-5189.
26. E. Le Roux, R. Malacea, E. Manoury, R. Poli, L. Gonsalvi and M. Peruzzini, *Adv. Synth. & Catal.*, 2007, **349**, 309-313.
27. E. Hauptman, R. Shapiro and W. Marshall, *Organometallics*, 1998,

17, 4976-4982.
28. E. Hauptman, P. J. Fagan and W. Marshall, *Organometallics*, 1999, **18**, 2061-2073.
29. S. Gladiali, F. Grepioni, S. Medici, A. Zucca, Z. Berente and L. Kollar, *Eur. J. Inorg. Chem.*, 2003, 556-561.
30. E. Guimet, M. Dieguez, A. Ruiz and C. Claver, *Dalton Trans.*, 2005, 2557-2562.
31. R. Malacea, E. Manoury, L. Routaboul, J.-C. Daran, R. Poli, J. P. Dunne, A. C. Withwood, C. Godard and S. B. Duckett, *Eur. J. Inorg. Chem.*, 2006, 1803–1816.
32. H. J. Drexler, W. Baumann, A. Spannenberg, C. Fischer and D. Heller, *J. Organomet. Chem.*, 2001, **621**, 89-102.
33. A. Preetz, H. J. Drexler, C. Fischer, Z. Dai, A. Borner, W. Baumann, A. Spannenberg, R. Thede and D. Heller, *Chem. Eur. J.*, 2008, **14**, 1445-1451.
34. A. Preetz, C. Fischer, C. Kohrt, H. J. Drexler, W. Baumann and D. Heller, *Organometallics*, 2011, **30**, 5155-5159.
35. I. D. Gridnev, E. Alberico and S. Gladiali, *Chem. Commun.*, 2012, **48**, 2186-2188.
36. T. Hayashi, T. Mise, M. Fukushima, M. Kagotani, N. Nagashima, Y. Hamada, A. Matsumoto, S. Kawakami, M. Konishi, K. Yamamoto and M. Kumada, *Bull. Chem. Soc. Japan*, 1980, **53**, 1138-1151.
37. A. Altomare, M. Burla, M. Camalli, G. Cascarano, C. Giacovazzo, A. Guagliardi, A. Moliterni, G. Polidori and R. Spagna, *J. Appl. Cryst.*, 1999, **32**, 115-119.
38. G. M. Sheldrick, *Acta Cryst. A*, 2008, **64**, 112-122.
39. M. N. Burnett and C. K. Johnson, *ORTEPIII, Report ORNL-6895.* , Oak Ridge National Laboratory, Oak Ridge, Tennessee, U.S. , 1996.
40. L. J. Farrugia, *J. Appl. Crystallogr.*, 1997, **30**, 565.
41. M. J. Frisch, G. W. Trucks, H. B. Schlegel, G. E. Scuseria, M. A. Robb, J. R. Cheeseman, G. Scalmani, V. Barone, B. Mennucci, G. A. Petersson, H. Nakatsuji, M. Caricato, X. Li, H. P. Hratchian, A. F. Izmaylov, J. Bloino, G. Zheng, J. L. Sonnenberg, M. Hada, M. Ehara, K. Toyota, R. Fukuda, J. Hasegawa, M. Ishida, T. Nakajima, Y. Honda, O. Kitao, H. Nakai, T. Vreven, J. Montgomery, J. A., J. E. Peralta, F. Ogliaro, M. Bearpark, J. J. Heyd, E. Brothers, K. N. Kudin, V. N. Staroverov, R. Kobayashi, J. Normand, K. Raghavachari, A. Rendell, J. C. Burant, S. S. Iyengar, J. Tomasi, M. Cossi, N. Rega, N. J. Millam, M. Klene, J. E. Knox, J. B. Cross, V. Bakken, C. Adamo, J. Jaramillo, R. Gomperts, R. E. Stratmann, O. Yazyev, A. J. Austin, R. Cammi, C. Pomelli, J. W. Ochterski, R. L. Martin, K. Morokuma, V. G. Zakrzewski, G. A. Voth, P. Salvador, J. J. Dannenberg, S. Dapprich, A. D. Daniels, Ö. Farkas, J. B. Foresman, J. V. Ortiz, J. Cioslowski and D. J. Fox, *Gaussian 09, Revision A.02*, Gaussian, Inc., Wallingford CT, 2009.
42. A. D. Becke, *J. Chem. Phys.*, 1993, **98**, 5648-5652.
43. C. T. Lee, W. T. Yang and R. G. Parr, *Phys. Rev. B*, 1988, **37**, 785-789.
44. D. Andrae, U. Haussermann, M. Dolg, H. Stoll and H. Preuss, *Theor. Chim. Acta*, 1990, **77**, 123-141.
45. U. Haussermann, M. Dolg, H. Stoll, H. Preuss, P. Schwerdtfeger and R. M. Pitzer, *Mol. Phys.*, 1993, **78**, 1211-1224.
46. W. Kuchle, M. Dolg, H. Stoll and H. Preuss, *J. Chem. Phys.*, 1994, **100**, 7535-7542.
47. T. Leininger, A. Nicklass, H. Stoll, M. Dolg and P. Schwerdtfeger, *J. Chem. Phys.*, 1996, **105**, 1052-1059.
48. A. W. Ehlers, M. Bohme, S. Dapprich, A. Gobbi, A. Hollwarth, V. Jonas, K. F. Kohler, R. Stegmann, A. Veldkamp and G. Frenking, *Chem. Phys. Lett.*, 1993, **208**, 111-114.
49. R. Malacea, E. Manoury, J.-C. Daran and R. Poli, *J. Mol. Struct.*, 2008, **890**, 249-254.
50. R. Malacea, L. Routaboul, E. Manoury, J.-C. Daran and R. Poli, *J. Organomet. Chem*, 2008, **693**, 1469–1477.
51. L. Diab, J. C. Daran, M. Gouygou, E. Manoury and M. Urrutigoity, *Acta Cryst. C*, 2007, **63**, M586-M588.
52. F. Teixidor, R. Benakki, C. Vinas, R. Kivekas and R. Sillanpaa, *Organometallics*, 1998, **17**, 4630-4633.
53. D. A. Evans, F. E. Michael, J. S. Tedrow and K. R. Campos, *J. Am. Chem. Soc.*, 2003, **125**, 3534-3543.
54. N. Khiar, R. Navas, E. Alvarez and I. Fernandez, *Arkivoc*, 2008, 211-224.
55. N. Khiar, R. Navas, B. Suarez, E. Alvarez and I. Fernandez, *Org. Lett.*, 2008, **10**, 3697-3700.
56. J. Browning, G. W. Bushnell, K. R. Dixon and R. W. Hilts, *J. Organomet. Chem.*, 1993, **452**, 205-218.
57. J. W. Faller, S. C. Milheiro and J. Parr, *J. Organomet. Chem.*, 2008, **693**, 1478-1493.
58. J. Browning, K. R. Dixon, N. J. Meanwell and F. Wang, *J. Organomet. Chem.*, 1993, **460**, 117-126.
59. H. S. Lee, J. Y. Bae, D. H. Kim, H. S. Kim, S. J. Kim, S. Cho, J. Ko and S. O. Kang, *Organometallics*, 2002, **21**, 210-219.
60. A. Neveling, G. R. Julius, S. Cronje, C. Esterhuysen and H. G. Raubenheimer, *Dalton Trans.*, 2005, 181-192.
61. J. A. Mata, A. R. Chianese, J. R. Miecznikowski, M. Poyatos, E. Peris, J. W. Faller and R. H. Crabtree, *Organometallics*, 2004, **23**, 1253-1263.
62. M. V. Baker, S. K. Brayshaw, B. W. Skelton, A. H. White and C. C. Williams, *J. Organomet. Chem.*, 2005, **690**, 2312-2322.
63. R. J. Lowry, M. K. Veige, O. Clement, K. A. Abboud, I. Ghiviriga and A. S. Veige, *Organometallics*, 2008, **27**, 5184-5195.
64. J. J. Robertson, A. Kadziola, R. A. Krause and S. Larsen, *Inorg. Chem.*, 1989, **28**, 2097-2102.
65. M. Toganoh, N. Harada and H. Furuta, *J. Organomet. Chem.*, 2008, **693**, 3141-3150.
66. H. F. Haarman, F. R. Bregman, J. M. Ernsting, N. Veldman, A. L. Spek and K. Vrieze, *Organometallics*, 1997, **16**, 54-67.
67. L. H. Gade, V. César and S. Bellemin-Laponnaz, *Angew. Chem. Engl.*, 2004, **43**, 1014-1017.
68. V. César, S. Bellemin-Laponnaz and L. H. Gade, *Eur. J. Inorg. Chem.*, 2004, 3436-3444.
69. V. César, S. Bellemin-Laponnaz, H. Wadepohl and L. H. Gade, *Chem. Eur. J.*, 2005, **11**, 2862-2873.
70. M. Stradiotto, J. Cipot and R. McDonald, *J. Am. Chem. Soc.*, 2003, **125**, 5618-5619.
71. A. D. Phillips, S. Bolaño, S. S. Bosquain, J.-C. Daran, R. Malacea, M. Peruzzini, R. Poli and L. Gonsalvi, *Organometallics*, 2006, **25**, 2189-2200.
72. M. Ahlmann and O. Walter, *J. Organomet. Chem.*, 2004, **689**, 3117-3131.
73. A. M. Z. Slawin, M. B. Smith and J. D. Woollins, *J. Chem. Soc., Dalton Trans.*, 1996, 1283-1293.
74. A. M. Z. Slawin, M. B. Smith and J. D. Woollins, *J. Chem. Soc., Dalton Trans.*, 1996, 4575-4581.